Band engineering in nanowires: *Ab initio* model of band edges modified by (111) biaxial strain in group IIIA-VA semiconductors

Eugene S. Kadantsev,[1,2,*] Michał Zieliński,[3] and Pawel Hawrylak[1]

[1]*Quantum Theory Group, Institute for Microstructural Sciences, National Research Council, Ottawa, Canada K1A 0R6*

[2]*Department of Chemistry, University of Ottawa, Ottawa, Canada K1N 6N5*

[3]*Instytut Fizyki UMK, Grudziądzka 5, 87-100 Toruń, Poland*

(Received 22 March 2012; revised manuscript received 18 May 2012; published 6 August 2012)

Quantum dots in nanowires grow on a (111) substrate and it is expected that the modifications of the band structure due to a biaxial strain in the (111) crystallographic plane will determine the confinement of charge carriers in these systems. In this work, we develop an *ab initio* methodology for the determination of biaxial strain-modified band energies on an absolute energy scale due to a strain in an *arbitrary* crystallographic plane and apply it to calculate the evolution of band edges in group IIIA-VA zinc-blende semiconductors (InP, InAs, and GaAs) under the (111) biaxial strain. The absolute hydrostatic deformation potentials, a prerequisite for the accurate calculation of the strain-modified band energies within our scheme, are determined. The strain tensor for an InAs dot grown on a (111) GaAs substrate is calculated and the importance of the (111) biaxial strain is demonstrated. The strained band offsets in InAs under a compressive biaxial strain in the (001) and (111) crystallographic planes as well as the local band structure in a InAs/GaAs dot indicates a stronger confinement of holes in the (111) case.

DOI: 10.1103/PhysRevB.86.085411 PACS number(s): 81.07.Gf, 71.20.Nr, 81.07.Ta, 81.05.Ea

I. INTRODUCTION

The electronic band structure of a semiconductor is modified by strain as described by the Bir-Pikus Hamiltonian (BPH)[1] and "model solid theory" (MST).[2] The deformation potentials and natural band offsets which enter these models determine the depth of "quantum confinement" in epitaxial semiconductor heterostructures which, in turn, determines their electronic and optical properties.

Significant progress has been achieved in *ab initio* calculations of the absolute hydrostatic deformation potentials (ADPs)[2–8] and natural band offsets (NBOs).[2,4,9–11] While the major difficulty associated with the calculation of these quantities—the definition of an absolute energy reference with periodic boundary conditions (PBC)—is overcome,[4,6–8,11] some quantitative differences remain.

This work is motivated by the fact that (i) in epitaxially grown heterostructures strains other than a pure hydrostatic strain might be important and (ii) the BPH/MST model is a perturbation theory and is valid only for small strains. A "variational" or "nonperturbative" treatment of the response of the band structure to a (001) biaxial strain was proposed in Ref. 12 (see also Ref. 13). An important step for the determination of strain-modified band edges was taken in Ref. 8, where it was proposed to correct the band energies[12,13] to account for the strain-dependent relaxation of a "reference level" in calculations with PBC. In the case of a compressive (001) biaxial strain applied to type I heterostructure, for example, an InAs dot on the (001) GaAs substrate, these corrections decrease (increase) the confinement for holes (electrons) by downshifting the band edges [Fig. 1(a)] inside the dot material (InAs).

Recently, III-V semiconductor nanowires[14–19] attracted considerable attention due to their applications in, for example, photonics[15,19] and photovoltaics.[17] Quantum dots (QDs) in nanowires are known to grow on the (111) substrate[14,19] and it is expected that (111) biaxial strain-modified band energies are important for these systems. In addition, quantum dots grown on a (111) substrate are expected[20,21] to have a vanishing "bright" exciton fine structure splitting[22] and lead to an efficient source of the entangled photons.[23,24] It is, therefore, important to extend the nonperturbative *ab initio* treatment of strain-modified band energies for an arbitrary crystallographic plane and, especially, for the (111) plane.

In this work, we develop methodology for the determination of band energies on an absolute energy scale due to a biaxial strain in an *arbitrary* crystallographic plane and carry out first-principles calculation of the (111) biaxial strain-modified band edges in group IIIA-VA semiconductors (InP, InAs, GaAs) with a zinc-blende (ZB) lattice structure. We reexamine the absolute hydrostatic deformation potentials (ADPs) in InP, InAs, and GaAs and use the revised ADPs to derive the "core reference level" corrections.[8] Finally, we discuss the strained band offsets in InAs subjected to a compressive biaxial strain in the (111) and (001) crystallographic planes, a situation encountered for an InAs quantum dot grown inside GaAs and InP nanowires. We demonstrate the importance of the (111) biaxial strain by atomistically computing the strain tensor inside an InAs dot grown on the (111) and (001) GaAs substrates and use the results of our *ab initio* calculations to derive the spatially varying local band profile inside the dot. The determined band offsets and local band structure in the strained quantum dot indicate a different confinement of holes in the (111) and (001) cases which opens an exciting possibility of engineering energy levels in nanostructures with strain.

II. METHODOLOGY

To calculate the biaxial strain-modified band edges due to a strain in an *arbitrary* crystallographic plane, we consider a "canonical coordinate system" defined by unit vectors $\mathbf{e}_1$ $\mathbf{e}_2$ $\mathbf{e}_3$

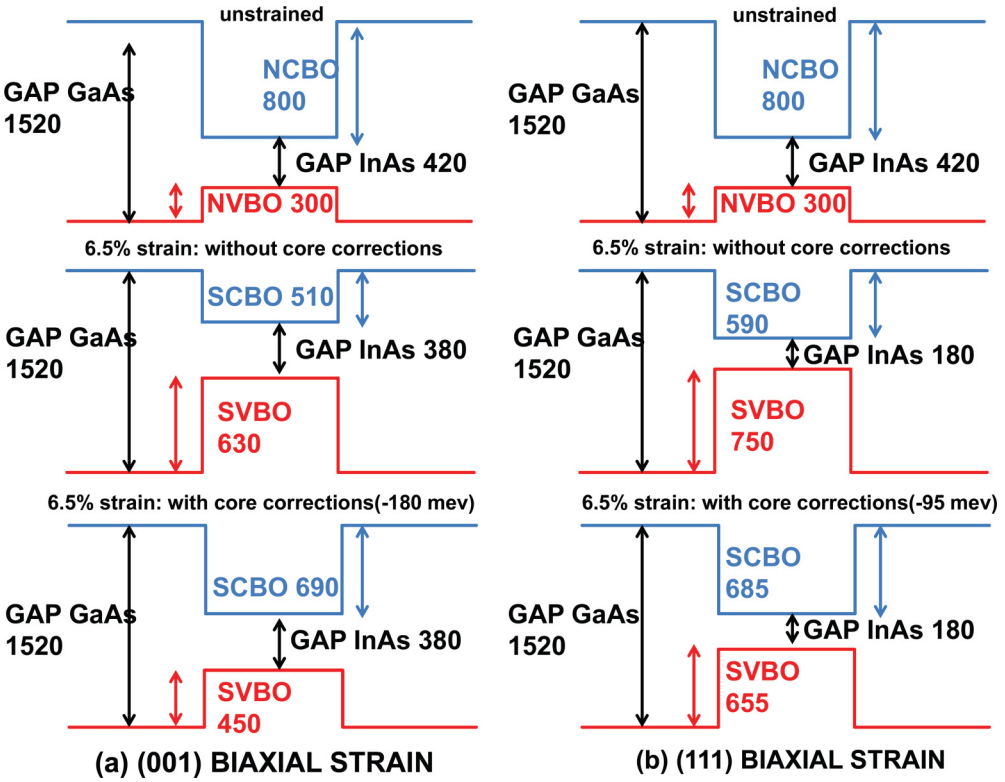

FIG. 1. (Color online) Strained valence and conduction band offsets (SVBO/SCBO) in InAs subjected to 6.5% compressive biaxial strain in the (001) (a) and (111) (b) crystallographic planes, respectively. The "core reference level" corrections decrease (increase) the confinement of holes (electrons). A combination of uncorrected band edges with large natural band offsets will result in the localization of holes that is too strong.[8] The natural valence band offset (NVBO) is taken to be 300 meV which, approximately, corresponds to GaAs matrix.

in which the strain tensor has the diagonal ("canonical") form,

$$\hat{\varepsilon}_D = \begin{pmatrix} \alpha & 0 & 0 \\ 0 & \alpha & 0 \\ 0 & 0 & -\nu\alpha \end{pmatrix}. \tag{1}$$

The unit vectors $\mathbf{e}_1$ and $\mathbf{e}_2$ span the plane in which the biaxial strain of magnitude α is applied, whereas vector $\mathbf{e}_3$ points in the perpendicular (out-of-plane) direction. The Poisson ratio[25] ν determines the response to the in-plane strain α. The canonical coordinate system can be obtained from the Cartesian coordinate system by an orthogonal transformation $\mathbf{T}$: $(\mathbf{e}_1,\mathbf{e}_2,\mathbf{e}_3)^T = \mathbf{T}(\mathbf{e}_x,\mathbf{e}_y,\mathbf{e}_z)^T$, where $\mathbf{T}$ is expressed through the crystallographic plane indices.[26–28] The biaxial strain tensor in the Cartesian coordinates ε_C is then obtained from the equation $\hat{\varepsilon}_C = \mathbf{T}^T\hat{\varepsilon}_D\mathbf{T}$. In the specific case of the (111) biaxial strain, the strain tensor is

$$\hat{\varepsilon}_B^{111} = \frac{\alpha}{3}\begin{pmatrix} 2-\nu & -1-\nu & -1-\nu \\ -1-\nu & 2-\nu & -1-\nu \\ -1-\nu & -1-\nu & 2-\nu \end{pmatrix}. \tag{2}$$

Note that after the transformation to the Cartesian coordinates, the biaxial strain tensor is still a function of just two variables α and ν.

Then, for a range of in-plane strains α, we determine the equilibrium geometries by minimizing the total energy. For each fixed in-plane strain α, we perform a series of density functional theory (DFT) total energy calculations using several trial values of ν. The internal atomic positions are allowed to relax in these calculations. As a result, for each in-plane strain α, one obtains a response $\nu(\alpha)$ (the Poisson ratio) and a set of the internal atomic coordinates which minimize the total energy. The procedure for the determination of the Poisson ratio follows that of Hammerschmidt *et al.*[28]

At the optimized geometry, we compute the band energies at the Γ point of the Brillouin zone with respect to a "reference level." In particular, we are interested in the energies of the conduction band minimum (CBM), heavy and light hole (HH/LH), and split-off (SO) bands. In our calculations, we choose the average of the cation (In,Ga)/anion(As,P) $1s$ core level energies as the reference $E_{\rm ref} = 1/2(E_{1s}^{\rm anion} + E_{1s}^{\rm cation})$. At this stage, we obtain the evolution of band energies with respect to the "core reference level" as a function of the in-plane strain α. To correct the DFT band gap error, we apply the scissor operator to restore the experimental band gap and split-off energy at zero strain.

The final step of our procedure is the correction of the band edges to account for the movement of the "core reference level" on the absolute energy scale under the biaxial strain.[8] The movement of the "core reference level" under the biaxial strain in the (klm) plane is the sum of the hydrostatic and uniaxial contributions,

$$dE_{\rm ref} = ((1+\alpha)^3 - 1)a_V^{1s} + (-\nu\alpha - \alpha)\,a_V^{1s/klm}. \tag{3}$$

This shift of the "core reference level" [Eq. (3)] is a function of the absolute hydrostatic and uniaxial deformation potentials

(a_V^{1s} and $a_V^{1s/klm}$, respectively) and the in-plane and out-of-plane strains (α and ν). The deformation potentials in Eq. (3) are determined through the supercell calculations.[6–8]

All the calculations in this work are carried out using the Kohn-Sham form of density functional theory (KS DFT)[29,30] in the local spin density approximation (LSDA)[31] and the augmented plane wave plus local orbitals (APW + lo) method.[32,33] The core levels are treated fully relativistically and self-consistently in the spherical approximation, whereas the valence states are treated using the second-variational Hamiltonian.[34,35] The Perdew-Wang[36] parametrization of the correlation energy is employed. The EXC!TING APW + LO program[37] is used. The local orbitals and linearization energies are taken from the program's database. The parameter $R_{\mathrm{MT}} \times K_{\max}$ which determines the "size" of the plane wave basis set is set to 8.0, where $K_{\max}$ is related to the kinetic energy cutoff ($K_{\max}^2/2$) and $R_{\mathrm{MT}} = 2$ a.u. is the muffin-tin radius. The reciprocal space is sampled with $\{11 \times 11 \times 11\}$ and $\{6 \times 6 \times 1\}$ **k** points in the case of the primitive (two-atom) unit cell and 48-atom supercell, respectively. Due to the high cost of the all-electron calculations with spin-orbital coupling, the supercell geometry optimizations are carried out using the plane wave pseudopotential approach[38] as implemented in the ABINIT program.[39,40]

III. ABSOLUTE DEFORMATION POTENTIALS

An absolute (volume) deformation potential (ADP) is defined for a specific band and type of strain and describes the band's change in energy with the relative volume change $a_V^{\mathrm{BAND}} = dE^{\mathrm{BAND}}/dln(V)$. In our work, the positive (negative) deformation potential always means that the band's energy increases (decreases) with increasing (decreasing) volume. One can also define the deformation potential of the band gap $a_V^{\mathrm{GAP}} = d(E^{\mathrm{CBM}} - E^{\mathrm{VBM}})/dln(V) = a_V^{\mathrm{CBM}} - a_V^{\mathrm{VBM}}$, where a_V^{CBM} and a_V^{VBM} are the deformation potentials of the conduction band minimum (CBM) and valence band maximum (VBM). Note that our notation is different from that of Vurgaftman *et al.*,[41] who reverses the sign of the deformation potential of the valence band maximum and defines the deformation potential of the band gap as $a_V^{\mathrm{GAP}} = a_V^{\mathrm{CBM}} + a_V^{\mathrm{VBM}}$.

One of the major difficulties in the calculation of ADPs is the definition of the absolute energy scale in the PBC calculations. Whereas the energy difference of two levels in the same PBC calculation is a well-defined quantity, the energy difference of two levels from two different PBC calculations is not, as the electron density and the total energy are invariant with respect to the rigid potential shift. One can use supercell calculations to establish a common energy reference.

To calculate the hydrostatic and uniaxial deformation potentials required to correct the biaxial strain-modified band edges [Eq. (3)], we follow the procedure outlined in Refs. 6–8. We construct 48 atom supercells with ⟨001⟩, ⟨110⟩, and ⟨111⟩ growth direction. The ⟨001⟩ and ⟨111⟩ supercells contain 12 cation-anion monolayers and it has been previously demonstrated[6,7] that these supercells are large enough to obtain 0.1 eV convergence of the deformation potentials. In the case of polar orientations (⟨111⟩ and ⟨001⟩), the anion- and cation-terminated supercells are constructed. Then, one-half of these supercells is either compressed or elongated by 1% in the growth direction, whereas the other half remains unstrained. The uniaxial deformation potentials are computed from the energy differences of the "core levels" that are spatially localized in the strained and unstrained part of the supercell.[6–8] The compressive and tensile uniaxial deformation potentials are averaged. Once the uniaxial deformation potentials are calculated, the absolute hydrostatic potentials (ADPs) obtained by the spherical averaging procedure.[6] In total, we perform 10 supercell calculations for each semiconductor (InAs, GaAs, and InP).

TABLE I. The absolute uniaxial and hydrostatic deformation potentials (in eV) of the "core reference level" for InAs, InP, and GaAs zinc-blende semiconductors (eV) obtained from supercell calculations as described in this work.

$a_V^{1s/001}$	$a_V^{1s/110}$	$a_V^{1s/111}$	a_V^{1s}
	InAs		
1.40	2.14	2.56	2.03
	InP		
1.03	1.32	2.15	1.45
	GaAs		
1.96	2.76	2.91	2.57

In our previous work,[8] the deformation potentials were calculated by assuming that the internal atomic positions $\mathbf{R}_i$ in the the supercell are completely determined by the strain tensor $\mathbf{R}_i = (\hat{1} + \hat{\varepsilon})\mathbf{R}_{i,0}$, where $\mathbf{R}_{i,0}$ are atomic positions in the unstrained zinc-blende lattice. In this work, the deformation potentials were reexamined to account for the strain-induced internal displacements within the supercell.[42] To accomplish this, the atomic positions within the supercell are relaxed while the atoms at the strained/unstrained interface are kept fixed. The supercell geometries with the relaxed internal atomic positions are then used as an input to the all-electron APW + LO calculation of the uniaxial deformation potentials. We find that ⟨110⟩, and especially ⟨111⟩, uniaxial deformation potentials are strongly affected by the internal atomic position relaxations, whereas the ⟨001⟩ uniaxial deformation potential is not affected. The internal relaxation results in an increase of ⟨110⟩ and ⟨111⟩ uniaxial deformation potentials by 0.2–0.4 eV and 0.8–1.0 eV, respectively.

Our uniaxial and hydrostatic deformation potentials of the "core reference level" obtained from the supercell calculations are summarized in Table I for InAs, GaAs, and InP zinc-blende semiconductors. The ADP of the valence band maximum (VBM) a_V^{VBM} and conduction band minimum (CBM) a_V^{CBM} can be derived from the core deformation potentials (Table I) using the equations $a_V^{\mathrm{VBM}} = a_V^{\mathrm{VBM}/1s} + a_V^{1s}$ and $a_V^{\mathrm{CBM}} = a_V^{\mathrm{CBM}/1s} + a_V^{1s}$, where $a_V^{\mathrm{VBM}/1s}$ and $a_V^{\mathrm{CBM}/1s}$ are well-defined deformation potentials of VBM and CBM with respect to the "core reference level." Table II summarizes our revised ADPs for CBM and VBM in InAs, GaAs, and InP, and results from the literature. Table II shows a good agreement between our deformation potentials and those of Li *et al.*[7] In the case of the VBM ADP, the differences are of the order 0.6 eV. It is to be noted, however, that the two sets of calculations differ in the

TABLE II. The absolute deformation potentials (ADPs) (in eV) of the conduction band minimum a_V^{CBM}, valence band maximum a_V^{VBM}, and of the direct Γ-point band gap $a_V^{\mathrm{CBM}} - a_V^{\mathrm{VBM}}$ for InAs, InP, and GaAs zinc-blende semiconductors.

METHOD	a_V^{CBM}	a_V^{VBM}	$a_V^{\mathrm{CBM}} - a_V^{\mathrm{VBM}}$
	InAs		
This work[a]	−3.83	1.20	−5.03
Ref. 8[b]	−4.31	0.72	−5.03
MST[c]	−5.08	1.00	−6.08
LAPW[d]	−3.87	1.79	−5.66
Exp.[e]			−6.0
	InP		
This work[a]	−4.15	1.28	−5.43
Ref. 8[b]	−4.45	0.98	−5.43
MST[c]	−5.04	1.27	−6.31
LAPW[d]	−4.10	1.83	−5.93
Exp.[e]			−6.6
	GaAs		
This work[a]	−5.64	1.77	−7.41
Ref. 8[b]	−6.24	1.17	−7.41
MST[c]	−7.17	1.16	−8.33
LAPW[d]	−5.91	2.24	−8.15
Exp.[e]			−8.5

[a]This work (the internal atomic positions were allowed to relax).
[b]Reference 8 (the internal atomic positions were "frozen").
[c]Model solid theory (Ref. 2).
[d]Linearized augmented plane wave (LAPW) calculations of Li *et al.* (Ref. 7).
[e]Experiment.[41]

treatment of the supercell geometries and relativity and this may account for the discrepancy.

IV. (111) BIAXIAL STRAIN-MODIFIED BAND EDGES (BBES)

The evolution of the CBM, heavy hole (HH), light hole (LH), and split-off (SO) energy bands on an absolute energy scale (including the "core reference level" corrections) as a function of the in-plane (111) biaxial strain α is shown on Fig. 2 for InAs (a), InP (b), and GaAs (c), respectively. In the case of InAs, we also show the (001) biaxial strain-modified band edges on the same plot [Fig. 2(a), solid red squares] for comparison.

TABLE III. Fit coefficients obtained by fitting the (111) biaxial strain-modified band edges to a polynomial of 3rd degree in the in-plane biaxial strain (α).

BAND	C_0	C_1	C_2	C_3
		InAs		
CBM	420	−7110.19	−1668.16	1266540
HH	0	−2836.29	48349.1	88050.7
LH	0	3935.14	87049.3	−225851
SO	−380	2224.37	−112456	2224.37
		InP		
CBM	1420	−6776.07	−60889.9	756456
HH	0	−3041.74	20802.2	−172488
LH	0	1810.82	113432	122546
SO	−110	2832.2	−176838	−859840
		GaAs		
CBM	1520	−9309.87	−46276.3	922039
HH	0	−1643.79	16041.5	−359250
LH	0	4977.83	63558.4	−349395
SO	−340	2722.8	−139587	−317536

For each band, the (111) biaxial strain-modified band edges are fitted to a polynomial of third degree in strain $E^{\mathrm{BAND}}_{\mathrm{BIAXIAL}} = C_{0\mathrm{BAND}} + C_{1\mathrm{BAND}}\alpha + C_{2\mathrm{BAND}}\alpha^2 + C_{3\mathrm{BAND}}\alpha^3$. The fit coefficients are summarized in Table III to enable strain parametrization of the empirical tight-binding and pseudopotential models. The fit is visualized in Fig. 2 as solid black curves going through numerical data (empty boxes). Overall, we find that our fit is quite good. The "core reference level" corrections [Eq. (3)] shift all the bands up or down in energy. The magnitude of the shift depends on the strain tensor (α and ν) and the uniaxial and hydrostatic deformation potentials (Table I). In the case of 6.5% compressive (111) ((001)) biaxial strain in InAs, the InAs bands are shifted down by 95 (180) meV (Fig. 1). The magnitude of the downshift is

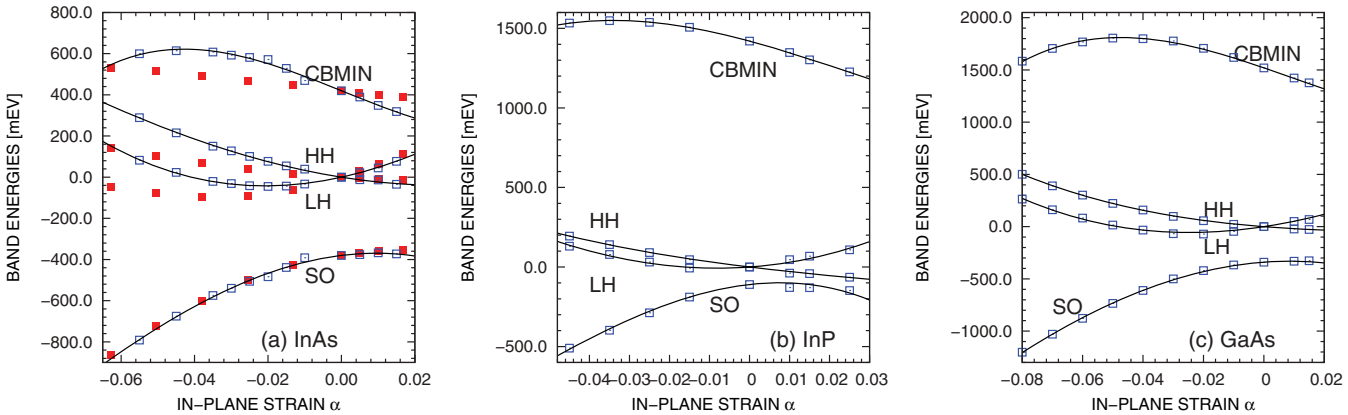

FIG. 2. (Color online) The absolute (111) biaxial strain-modified band edges (BBEs) as a function of the in-plane strain ε. The black solid lines are a fit to the numerical data (empty boxes). CBM - conduction band minimum; HH/LH - heavy and light holes; SO - the split-off band. For InAs, the (001) biaxial strain-modified band edges are shown for comparison (solid red squares).

smaller in the (111) case due to the fact that the (111) uniaxial deformation potential is larger.

Under the compressive (111) biaxial strain, the top of the valence band goes up, whereas the split-off band goes down (Fig. 2). The bottom of the conduction band (CBM) goes up in energy for $\alpha < 0.04$ (Fig. 2). At 2–4% compressive strain and for larger strains, we find strong nonlinearities in the behavior of the conduction and valence bands. The CBM nonlinearity is especially strong as the CBM energy goes up and, then, down in energy (Fig. 2). It is interesting to note that at 6% strain, the absolute energy of the InAs CBM is close in value in the case of the (111) and (001) strains [Fig. 2(a)]. We note that the ADPs are fixed in the model solid theory and the linear dependence on strain will strongly overestimate the changes in the CBM energy.

Motivated by reports of the nanowire growth in the ⟨001⟩[43,44] as well as ⟨111⟩ directions,[19] we compare the strained band offsets for biaxial strains in the (001) and (111) crystallographic planes. The strained band offset between two semiconductors is the sum of the natural band offset between "strain-free" semiconductors and the biaxial strain-induced corrections.

Comparing the InAs valence bands for the (001) and (111) biaxial strains [Fig. 2(a)], we find that the HH band at 6.5% (111) biaxial strain (a situation encountered for a InAs dot in GaAs nanowire) is higher by 200 meV than the HH band at 6.5% (001) strain. Figures 1(a) and 1(b) show the absolute band energies in InAs subjected to 6.5% compressive biaxial strain in the (001) and (111) crystallographic planes, respectively, a situation encountered in a InAs quantum dot grown inside a GaAs nanowire. We find that (1) the strained valence band offsets (SVBOs) are smaller than conduction band offsets (SCBOs) which may indicate stronger susceptibility of holes to strain; (2) at 6.5% strain, the SVBO for holes is larger by 200 meV in the case of the (111) biaxial strain (655 meV vs 450 meV) which indicates a stronger confinement for holes in the (111) case. Note that the core corrections account only for one-half of the 200 meV (i.e., the effect of a deeper confining potential for holes is already present in the "uncorrected" band edges and the core corrections act to enhance this effect).

At 3% compressive strain, a situation encountered for InAs dots grown inside the InP nanowire, the strain-induced modification of the band edges is less pronounced. As for 6.5% strain, the holes are more confined in the (111) case but the differences are smaller (the confinement is stronger by 80 meV vs 200 meV). The CBM in the (111) case lies higher by 120 meV than in the (001) case indicating a somewhat weaker confinement in the former case.

V. InAs DOT INSIDE GaAs NANOWIRE

To illustrate the confinement of charge carriers in heterostructures strained in the (001) and (111) crystallographic planes such as quantum dots in nanowires, we performed valence force field geometry optimization of a InAs disk-shaped quantum dot (QD) with radius $R = 17$ lattice constants (l.c.) and height $H = 5$ l.c. grown on the (111) and (001) substrate inside the GaAs matrix. This was followed by the atomistic determination of the local strain tensor. We model the "dot" and "nanowire" using a zinc-blende and not wurtzite

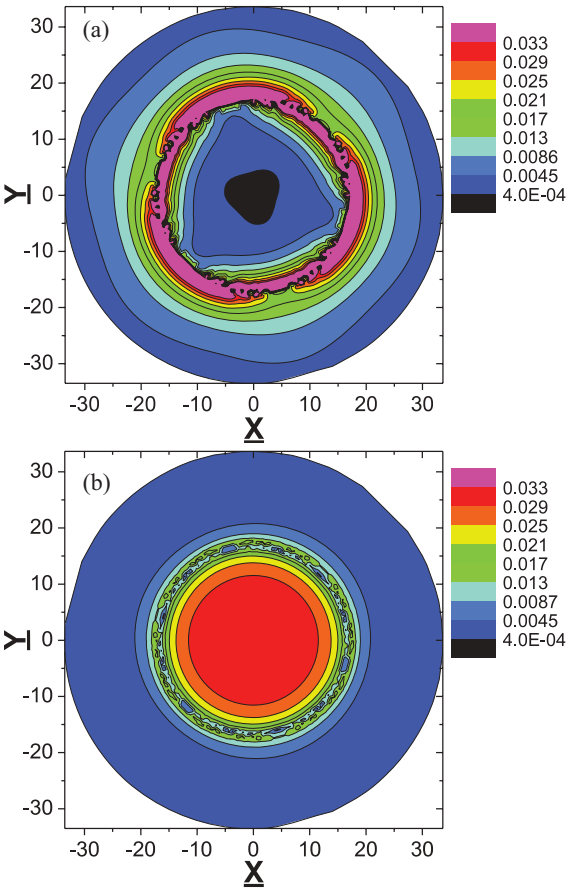

FIG. 3. (Color online) Two functions of strain tensor for a InAs disk quantum dot grown on the (111) GaAs substrate in the plane parallel to the substrate: $B_D(\mathbf{e}) = \sqrt{(\varepsilon_{xx} - \varepsilon_{yy})^2 + (\varepsilon_{yy} - \varepsilon_{zz})^2 + (\varepsilon_{zz} - \varepsilon_{xx})^2}$ (a) and $B_{111}(\mathbf{e}) = (\varepsilon_{xy} + \varepsilon_{yz} + \varepsilon_{zx})/3$ (b). Distances are in lattice constants.

structure, but expect that our qualitative conclusions will be valid for both phases, as those two phases vary only in the position of the second nearest neighbor, while the symmetry in both systems is identical.[21]

For the QD grown on the (111) substrate, Fig. 3 shows two functions of the strain tensor $B_D(\mathbf{e}) = \sqrt{(\varepsilon_{xx} - \varepsilon_{yy})^2 + (\varepsilon_{yy} - \varepsilon_{zz})^2 + (\varepsilon_{zz} - \varepsilon_{xx})^2}$ [Fig. 3(a)] and $B_{111}(\mathbf{e}) = (\varepsilon_{xy} + \varepsilon_{yz} + \varepsilon_{zx})/3$ [Fig. 3(b)] in the plane perpendicular to the dot's axis of symmetry. Figure 3(a) clearly shows a C_{3v} symmetry of the biaxial strain distribution. This result is consistent with the findings in the recent work by Singh and Bester[20] that C_{3v} symmetry is characteristic of the zinc-blende, wurtzite, or mixed phase systems grown on the (111) substrate. Function B_D [Fig. 3(a)] can also be thought of as a measure of the (001) biaxial strain which strongly affects the diagonal components of the strain tensor (see, e.g., Fig. 10 of Ref. 13). We find that for the QD grown on the (111) substrate, the (001) biaxial strain is small.

Figure 3(b) shows the average of the off-diagonal (shear) strain tensor element. The magnitude of this average reaches 3%—one-half of the InAs/GaAs lattice mismatch. This demonstrates a significant role of the (111) biaxial strain for systems grown on the (111) substrate. The distribution of the shear strain function is nearly cylindrical and reproduces

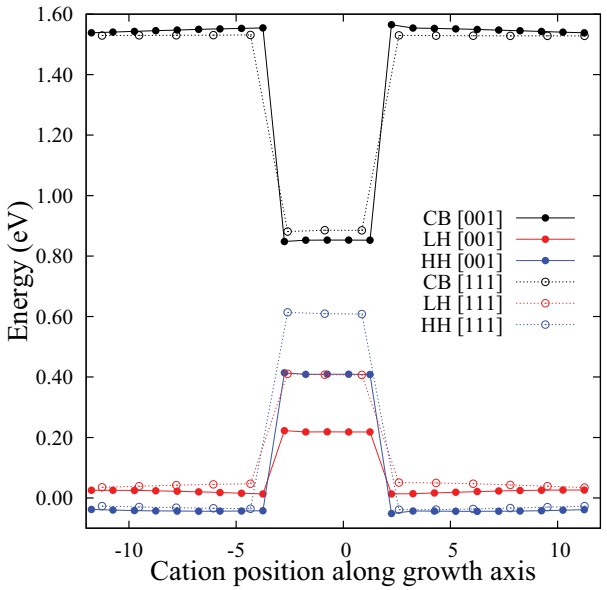

FIG. 4. (Color online) The local bandstructure in a InAs quantum dot grown on the (001) and (111) GaAs substrate. The band structure is plotted along the dot's axis and is calculated from the VFF strain tensor and BBEs computed in this work. The confinement of holes is stronger in the (111) case. Distances are in lattice constants.

the approximate cylindrical symmetry of the quantum dot's shape, rather than the C_{3v} symmetry of the underlying crystal lattice. We find that B_{111} is larger in the QD grown on the (111) substrate compared with the QD grown on the (001) substrate (not shown). We performed our calculation using different sets of the valence force field (VFF) parameters[45,46] and obtained very similar results, independent of the particular VFF parametrization. We speculate that the absolute values of the strain field should not vary significantly between the zinc-blende and wurtzite phases. Overall, we conclude that the (111) biaxial strain is important for dots grown on the (111) substrate and the (111) biaxial strain-modified band edges are important for the understanding of the confinement of charge carriers in these systems.

Then, we use the local strain tensor inside and in the vicinity of the InAs dot from the VFF calculation and the biaxial strain-modified band edges (BBEs) computed in this work to derive the local band structure[47] for the dot grown on the (001) and (111) substrate. This local band structure is shown in Fig. 4. We note that the different spacing of the cation atoms in Fig. 4 is due to the different spacing of the subsequent cation layers in the ⟨111⟩ and ⟨001⟩ directions. For both types of strain [(001) and (111)], we observe the reversal of the light and heavy hole band ordering in the dot/matrix region. The local band structure inherits the main features of the BBEs used to derive it and we find that the magnitude of the confining potential for holes is deeper by 200 meV in the case of the (111) biaxial strain.

VI. CONCLUSIONS

In conclusion, we have developed a nonperturbative *ab initio* methodology for the determination of the strain-modified band edges on an absolute energy scale due to a biaxial strain in an *arbitrary* crystallographic plane. The developed methodology was applied to InAs, InP, and GaAs zinc-blende semiconductors strained in the (111) plane, a situation encountered for quantum dots grown inside nanowires. The band edges were fitted to a polynomial of third degree in the in-plane strain and the fit coefficients were tabulated, thus, enabling the strain parametrization of the empirical tight binding and pseudopotential models. The importance of the (111) biaxial strain for quantum dots grown in nanowires was demonstrated through atomistic calculations. The strained band offset, a measure of confinement for charge carriers, was compared for InAs strained in the (001) and (111) crystallographic planes and a stronger localization of holes was found in the (111) case. Our methodology allows for computational experiments in the strain engineering of electron and hole energy levels in nanostructures.

ACKNOWLEDGMENTS

E. S. Kadantsev thanks the Government of Canada for establishing the National Research Council–Natural Sciences and Engineering Research Council–Business Development Bank (NRC-NSERC-BDC) Nanotechnology partnership. M.Z. acknowledges support from the Foundation for Polish Science, Homing Plus Programme, cofinanced by the European Union within the European Regional Development Fund. The authors acknowledge discussions with M. Korkusiński, P. Poole, and D. Dalacu.

*ekadants@uottawa.ca

[1] G. L. Bir and G. E. Pikus, *Symmetry and Strain-Induced Effects in Semiconductors* (Wiley, New York, 1975).
[2] C. G. Van de Walle, Phys. Rev. B **39**, 1871 (1989).
[3] C. G. Van de Walle and R. M. Martin, Phys. Rev. Lett. **62**, 2028 (1989).
[4] A. Janotti and C. G. Van de Walle, Phys. Rev. B **75**, 121201 (2007).
[5] S.-H. Wei and A. Zunger, Phys. Rev. B **60**, 5404 (1999).
[6] Y.-H. Li, X. G. Gong, and S.-H. Wei, Appl. Phys. Lett. **88**, 042104 (2006).
[7] Y.-H. Li, X. G. Gong, and S.-H. Wei, Phys. Rev. B **73**, 245206 (2006).
[8] E. S. Kadantsev and P. Hawrylak, Appl. Phys. Lett. **98**, 023108 (2011).
[9] A. Baldereschi, S. Baroni, and R. Resta, Phys. Rev. Lett. **61**, 734 (1988).
[10] S.-H. Wei and A. Zunger, Appl. Phys. Lett. **72**, 2011 (1998).
[11] Y.-H. Li, A. Walsh, S. Chen, W.-J. Yin, J.-H. Yang, J. Li, J. L. F. Da Silva, X. G. Gong, and S.-H. Wei, Appl. Phys. Lett. **94**, 212109 (2009).
[12] P. R. C. Kent, G. L. W. Hart, and A. Zunger, Appl. Phys. Lett. **81**, 4377 (2002).
[13] E. S. Kadantsev, M. Zielinski, M. Korkusinski, and P. Hawrylak, J. Appl. Phys. **107**, 104315 (2010).

[14]J. Johansson, L. S. Karlsson, C. P. T. Svensson, T. Mårtensson, B. A. Wacaser, K. Deppert, L. Samuelson, and W. Seifert, Nat. Mater. **5**, 574 (2006).
[15]M. T. Borgstrom, V. Zwiller, E. Muller, and A. Imamoglu, Nano Lett. **5**, 1439 (2005).
[16]Y. M. Niquet, A. Lherbier, N. H. Quang, M. V. Fernández-Serra, X. Blase, and C. Delerue, Phys. Rev. B **73**, 165319 (2006).
[17]T. J. Kempa, B. Tian, D. R. Kim, J. Hu, X. Zheng, and C. M. Lieber, Nano Lett. **8**, 3456 (2008).
[18]H. Shtrikman, R. Popovitz-Biro, A. Kretinin, L. Houben, M. Heiblum, M. Bukala, M. Galicka, R. Buczko, and P. Kacman, Nano Lett. **9**, 1506 (2009).
[19]D. Dalacu, A. Kam, D. G. Austing, X. Wu, J. Lapointe, G. C. Aers, and P. J. Poole, Nanotechnology **20**, 1 (2009).
[20]R. Singh and G. Bester, Phys. Rev. Lett. **103**, 063601 (2009).
[21]A. Schliwa, M. Winkelnkemper, A. Lochmann, E. Stock, and D. Bimberg, Phys. Rev. B **80**, 161307(R) (2009).
[22]E. S. Kadantsev and P. Hawrylak, Phys. Rev. B **81**, 045311 (2010).
[23]A. J. Shields, Nature Photonics **1**, 215 (2007).
[24]R. M. Stevenson, R. J. Young, P. Atkinson, K. Cooper, D. A. Ritchie, and A. J. Shields, Nature (London) **439**, 179 (2006).
[25]G. N. Greaves, A. L. Greer, R. S. Lakes, and T. Rouxel, Nat. Mater. **10**, 823 (2011).
[26]P. M. Marcus and F. Jona, Phys. Rev. B **51**, 5263 (1995).
[27]D. N. Lee, Thin Solid Films **434**, 183 (2003).
[28]T. Hammerschmidt, P. Kratzer, and M. Scheffler, Phys. Rev. B **75**, 235328 (2007).
[29]P. Hohenberg and W. Kohn, Phys. Rev. **136**, B864 (1964).
[30]W. Kohn and L. J. Sham, Phys. Rev. **140**, A1133 (1965).
[31]U. von Barth and L. Hedin, J. Phys. C: Solid State Phys. **5**, 1629 (1972).
[32]E. Sjöstedt, L. Nordström, and D. J. Singh, Solid State Comm. **114**, 15 (2000).
[33]G. K. H. Madsen, P. Blaha, K. Schwarz, E. Sjöstedt, and L. Nordström, Phys. Rev. B **64**, 195134 (2001).
[34]D. D. Koelling and B. N. Harmon, J. Phys. C **10**, 3107 (1977).
[35]J. Kunes, P. Novak, R. Schmid, P. Blaha, and K. Schwarz, Phys. Rev. B **64**, 153102 (2001).
[36]J. P. Perdew and Y. Wang, Phys. Rev. B **45**, 13244 (1992).
[37]http://exciting.sourceforge.net; version 0.9.151.
[38]M. C. Payne, M. P. Teter, D. C. Allan, T. A. Arias, and J. D. Joannopoulos, Rev. Mod. Phys. **64**, 1045 (1992).
[39]X. Gonze, J.-M. Beuken, R. Caracas, F. Detraux, M. Fuchs, G.-M. Rignanese, L. Sindic, M. Verstraete, G. Zerah, F. Jollet *et al*., Comput. Mat. Sci. **25**, 478 (2002).
[40]X. Gonze, G.-M. Rignanese, M. Verstraete, J.-M. Beuken, Y. Pouillon, R. Caracas, F. Jollet, M. Torrent, G. Zerah, M. Mikami *et al*., Zeit. Kristallogr. **220**, 558 (2005).
[41]I. Vurgaftman, J. R. Meyer, and L. R. Ram-Mohan, J. Appl. Phys. **89**, 5815 (2001).
[42]L. Kleinman, Phys. Rev. **128**, 2614 (1962).
[43]M. T. Björk, B. J. Ohlsson, T. Sass, A. I. Persson, C. Thelander, M. H. Magnusson, K. Deppert, L. R. Wallenberg, and L. Samuelson, Appl. Phys. Lett. **80**, 1058 (2002).
[44]U. Krishnamachari, M. Borgstrom, B. J. Ohlsson, N. Panev, L. Samuelson, W. Seifert, M. W. Larsson, and L. R. Wallenberg, Appl. Phys. Lett. **85**, 2077 (2004).
[45]Y.-M. Niquet and D. C. Mojica, Phys. Rev. B **77**, 115316 (2008).
[46]Y. Cai and M. F. Thorpe, Phys. Rev. B **46**, 15879 (1992).
[47]C. Pryor, J. Kim, L. W. Wang, A. J. Williamson, and A. Zunger, J. Appl. Phys. **83**, 2548 (1998).